

# Electron Injection, Charge Recombination, and Energy Migration in Surface-Modified TiO<sub>2</sub> Nanocrystallite Layers. A Laser Photolysis Study

Joseph Rabani,<sup>\*,†</sup> Kiminori Ushida,<sup>‡</sup> Koichi Yamashita,<sup>‡</sup> Johannes Stark,<sup>†</sup>  
Shlomo Gershuni,<sup>†</sup> and Akira Kira<sup>‡</sup>

Department of Physical Chemistry and the Farkas Center, The Hebrew University of Jerusalem, Jerusalem 91904, Israel, and Chemical Dynamics Laboratory, The Institute of Physical and Chemical Research, Wako-shi, Saitama 351-01, Japan

Received: September 14, 1996; In Final Form: January 23, 1997<sup>®</sup>

Ru(bpy)<sub>3</sub><sup>2+</sup> (bpy ≡ bipyridine) and Ru(o-phen)<sub>3</sub><sup>2+</sup> (o-phen ≡ o-phenanthroline) have been adsorbed to a membrane layer made of TiO<sub>2</sub> nanocrystallites from aqueous solutions at pH 2.5 by means of pretreatment of the surface with Nafion, sodium dodecyl sulfate (SDS) or sodium dodecyl benzyl sulfate (SDBS). Pulsed laser-induced emission and absorbance changes have been studied. The time profiles provide information concerning environmental effects (charge and hydrophobic interactions) on the rates and yields of electron injection from the excited dyes to the TiO<sub>2</sub> membrane and subsequent electron recapture by Ru(III). The differences between the rates of electron injection and recapture, the multiexponential nature of these reactions, and the differences between specific photosensitizers and binders are discussed in light of the semiconducting properties of the TiO<sub>2</sub> nanocrystallites and the hydrophobic and ionic interactions between the photosensitizers and the binders. Oxidation of iodide ions by Ru(III) was also studied. Iodide ions react efficiently with Ru(III) despite the negative charge of the binders, indicating that most of the charge is neutralized by the surface charge of TiO<sub>2</sub> and by the Ru(III) ions. Quantum yields for net electron injection were determined from the initial (extrapolated) bleaching. In most systems observed bleaching corresponds to 30–80% of the absorbed photons. At relatively high laser pulse intensities, emission measurements show that bimolecular (and apparent higher order) processes take place, involving fast triplet annihilation. A detailed mechanism provides quantitative kinetic treatment of the data. Comparison of results in dry and wet layers indicates that energy migration is responsible for the enhanced triplet annihilation.

## Introduction

The present article concerns emission and bleaching kinetics and yields that are measured after pulsed laser excitation of Ru(bpy)<sub>3</sub><sup>2+</sup> and Ru(o-phen)<sub>3</sub><sup>2+</sup> adsorbed to a TiO<sub>2</sub> porous membrane by a polymer or surfactant binder.

Photochemistry and photoelectrochemistry of Ru complexes adsorbed to TiO<sub>2</sub> layers have been investigated by a number of laboratories. Interest in such systems increased remarkably after their role in vectorial charge migration had been demonstrated in the Graetzel cell.<sup>1–11</sup> This cell is based on a TiO<sub>2</sub> membrane layer made on an indium–tin-oxide (ITO) surface, to which a photosensitizer such as Ru(II)(dcbpy)<sub>3</sub><sup>4+</sup> (dc ≡ dicarboxy) is adsorbed. High quantum yields of photocurrents were reported as a result of illumination with visible light, using nonaqueous solutions of I<sup>−</sup>/I<sub>2</sub> for carrying the charge to the counter electrode. The proposed reaction mechanism involves electron injection from the photosensitizer into the conduction band of the semiconductor. The electron further migrates to the ITO electrode. The oxidized form of the Ru photosensitizer reacts with I<sup>−</sup> and produces iodine (I<sub>2</sub> in equilibrium with I<sub>3</sub><sup>−</sup>). The latter migrates to the counter electrode and is reduced by the electron which flows in the outer circuit.<sup>12</sup> A similar approach where the dyes are replaced by semiconductor nanocrystallites has been demonstrated by Gerischer and Lubke<sup>13a</sup> and by Weller and his co-workers<sup>13b</sup> on the basis of the pioneering works of Henglein et al. and subsequent investigations of Q-particles and sandwich colloids.<sup>14–33</sup> Films of nanocrystallites other than TiO<sub>2</sub> have also been studied.<sup>34–39</sup>

In the present article the adsorbed Ru complexes were used in a wet (contact with water) or in a dry state. The TiO<sub>2</sub> nanocrystallites were in the form of a solid porous membrane layer, possessing a positive charge at pH 2.5. The dyes used here are similar in their general properties to those used by Graetzel; however, since the photosensitizers used here are doubly charged positive ions, they can be adsorbed to the TiO<sub>2</sub> only after treating the TiO<sub>2</sub> surface with appropriate polymers or surfactants.<sup>40</sup> Similar surface modification as well as stabilization of semiconductor nanocrystallites by polymers and surfactants is well-known. Adsorption of ions such as ferri- and ferrocyanide by the negatively charged colloid particles of ZnO takes place in the presence of positive polyelectrolytes.<sup>41</sup> Controlling the physical properties of semiconductors (such as *E*<sub>cb</sub><sup>42</sup>) and rates of interfacial charge migration,<sup>43,44</sup> the concentration of electron and hole scavengers at the colloid particle surface,<sup>44</sup> and retarding photochemical back reactions<sup>45</sup> by polyelectrolytes have been previously reported.

## Experimental Section

**Materials.** Indium–tin oxide on glass plates (10 Ω per square) were bought from Geomatec. TiO<sub>2</sub> layers were prepared on the ITO surface using TiO<sub>2</sub> nanocrystallites dispersed in water at pH 2.5 (300 g/L, containing 1 wt % Triton X-100) by successive spin coatings followed by heating at 450 °C.<sup>5</sup> Usually 10 repeated coatings were used, with accumulated TiO<sub>2</sub> of 1 mg/cm<sup>2</sup>. The use of ITO as a support was a matter of convenience, as TiO<sub>2</sub> sticks easily to the ITO. No use was intended of the conduction properties of ITO. TiO<sub>2</sub> was prepared by hydrolysis of the respective propoxide at acid pH.

<sup>†</sup> The Hebrew University.

<sup>‡</sup> The Institute of Physical and Chemical Research.

<sup>®</sup> Abstract published in *Advance ACS Abstracts*, March 15, 1997.

Ru(bpy)<sub>3</sub><sup>2+</sup> (as a chloride) and Ru(o-phen)<sub>3</sub><sup>2+</sup> (as a chloride) were bought from Aldrich and used as received. Nafion (Aldrich, 5 wt % in a mixture of alcohols and water), sodium dodecyl sulfate (SDS, ultrapure grade, Baker), and sodium *n*-dodecyl benzene sulfonate (SDBS, Wako) were used as received. Other chemicals were of the highest available purity and were used without further purification. Water was deionized and distilled once.

The TiO<sub>2</sub> layers, typical dimensions 2.5 × 0.8 cm, were first equilibrated by shaking 48 h with 3 cm<sup>3</sup> of the polymer or surfactant solution. Typical solutions contained 0.17 M SDS or 0.1 M SDBS in 3 × 10<sup>-3</sup> M perchloric acid, or 0.75 wt % Nafion in 3 × 10<sup>-2</sup> M perchloric acid. The latter solution contained 14 wt % of the original alcohol mixture. Then the layers were washed with water and equilibrated by shaking 48 h with 3 cm<sup>3</sup> Ru(bpy)<sub>3</sub><sup>2+</sup> (2 × 10<sup>-4</sup> M) or Ru(o-phen)<sub>3</sub><sup>2+</sup> (1.5 × 10<sup>-4</sup> M) in 3 × 10<sup>-3</sup> M HClO<sub>4</sub>.

**Preparation of Samples for Illumination.** The glass plate carrying the TiO<sub>2</sub> layers was coupled with a bare plate of similar dimensions. The TiO<sub>2</sub> layer, usually loaded with the polymer or surfactant and with the Ru complex, was between the glass plates. The two plates were tightly held together by means of an appropriate slit at the Teflon base at the bottom of a four-windowed plastic cell. A specially fitted cover held the two plates tightly together at the top. The cell was flushed with Ar gas for at least 20 min prior to photolysis. Flushing for 15 h gave identical results whenever tested. A wet surface was obtained upon addition of 150 μL of air-free water or iodide solution. The liquid filled the space between the plates due to the capillary forces. In the case of Ru(bpy)<sub>3</sub><sup>2+</sup> in SDS-treated TiO<sub>2</sub>, the solution between the electrodes contained also 2 × 10<sup>-4</sup> M Ru(bpy)<sub>3</sub><sup>2+</sup>, in order to minimize desorption. Control experiments showed that the signals originating from the interplate solution were negligible, if any.

**Laser Photolysis.** A dye laser (Lumonix Hyper Dye 300), pumped by a Nd:YAG laser (Lumonix HY750), pulse width 8 ns, was used for excitation at 460 nm. The dye solution was 1.3 mM Coumarin 460 in methanol. The laser flash lamp was triggered at a 10 Hz rate, with the Q-switch being activated every 2–8 s. The laser beam, 3 mJ/pulse, was 2 mm in diameter. Lower intensities were obtained with the aid of appropriate neutral density filters. Emission was monitored at 605 nm, using Spex's Minimate monochromator equipped with a Hamamatsu R2083 photomultiplier. Several cutoff glass filters (Toshiba) were used to avoid the stray light from the exciting pulse. The response time (using 50 Ω termination) was 10 ns.

Transient bleaching was measured with the aid of the Hamamatsu R1913 highly linear photomultiplier with six dynodes and a Ritsu Oyo Kogaku Model MC10N monochromator. A xenon flash lamp (Eagle Shoji, SA200E) was used as an analytical light source. The layer samples were used at 45° to both the laser and the analytical light beams, the latter being perpendicular. A small piece of tag paper with a 1 mm pinhole was used in order to guarantee good overlap between the excitation and analytical beams. A second pinhole, a lens, and an interference filter were used between the sample and the monochromator to avoid scattered laser light. The response time (using 500 Ω termination) was 30 ns. A digital oscilloscope (Tektronix TD520) operated by an Epson PC286VG personal computer was used for data processing. Gated spectral measurements were performed using a spectral multichannel analyzer, a product of Princeton Instruments, Model IRY-700G/RB/par with PG100, equipped with a monochromator (Thermo Jarrell Ash, Monospec 27). The Xe flash lamp unit (SA200E) was used as a light source.

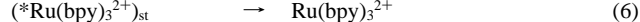
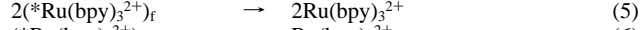
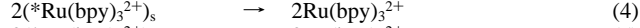
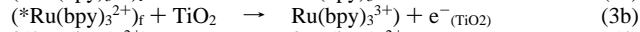
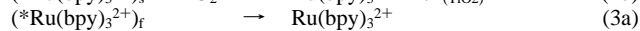
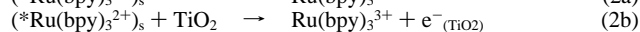
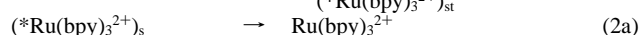
**Actinometry.** Actinometry was carried out using a 2 × 10<sup>-3</sup> M Ru(bpy)<sub>3</sub><sup>2+</sup> solution between glass plates at 0.21 mm distance, measuring the bleaching at 420 nm induced by the laser pulses. The light intensity was calculated using  $\epsilon(\text{Ru(bpy)}_3^{2+}) - \epsilon(*\text{Ru(bpy)}_3^{2+}) = 6.4 \times 10^6 \text{ mol}^{-1} \text{ cm}^2$ .<sup>46a</sup> The light intensity in the absence of cutoff neutral density light filters was 3.75 × 10<sup>-8</sup> einsteins/cm<sup>2</sup>. Lower intensities were obtained with the aid of appropriate neutral density filters between the laser source and the cell. The intensity of the emission light reaching the detector in a given system is proportional to the surface density of the excited dye (moles \*Ru(bpy)<sub>3</sub><sup>2+</sup> or \*Ru(o-phen)<sub>3</sub><sup>2+</sup> per cm<sup>2</sup>). It depends both on the photophysical and photochemical properties of the dye system and on the particular optical lineup. Since the amount of light scattering by the TiO<sub>2</sub> membrane changed from one sample to another, the factor converting the emitted light signal to surface density of the excited dye had to be determined for each of the systems.

## Results and Discussion

**Emission Decay Profiles.** All 12 possible combinations of TiO<sub>2</sub> layers treated with SDS, SDBS, or Nafion, loaded with Ru(bpy)<sub>3</sub><sup>2+</sup> or Ru(o-phen)<sub>3</sub><sup>2+</sup>, in the wet or the dry state were investigated. The time profiles of the emission at 605 nm were recorded in the range 2 ns to 3 μs, at five different laser beam intensities. The ratio of highest to lowest intensity was 103. The emission decay profiles show a buildup of the emission signal during the laser pulse (reaction 1) followed by a complex decay profile which can be fitted by two or three distinct decay processes. With the exception of the dry SDBS/Ru(o-phen)<sub>3</sub><sup>2+</sup> system, where the third decay amounts to 5%, in all other systems the first two stages account for >97% of the initial emission intensity. Each of the two major processes includes one-exponential decay in parallel with a second-order reaction. The latter is pronounced at the higher intensities used. Reactions 1–4 represent the mechanism according to which the time profiles in the Ru(bpy)<sub>3</sub><sup>2+</sup> systems were analyzed. Ru(o-phen)<sub>3</sub><sup>2+</sup> behaves similarly. Reaction 1 represents the excitation by the laser pulse. The three decay processes that follow were analyzed in terms of apparently different excited states, denoted as (\*Ru(bpy)<sub>3</sub><sup>2+</sup>)<sub>s</sub>, (\*Ru(bpy)<sub>3</sub><sup>2+</sup>)<sub>f</sub>, and (\*Ru(bpy)<sub>3</sub><sup>2+</sup>)<sub>st</sub>, responsible for the slow (reactions 2a,b and 4), fast (reactions 3a,b and 5), and slowest (reaction 6) decay processes, respectively. Surface reactions are known in many cases to have a distribution of lifetimes. It has been shown that two rate constants are sufficient to fit adequately one or two Gaussian distributions of lifetimes.<sup>46b</sup> As will be discussed later, in the present work the multiexponential decay of emission is attributed to hydrophobic and ionic interactions of the dye molecules with the binders affecting the spatial distribution of the molecules near the TiO<sub>2</sub> surface. The treatment of the kinetics in terms of two major exponential decays is useful for comparison of different systems and relating the results to the properties of the binders. It is likely that the two or three exponential decays represent one or two broad lifetime distributions, the nature of which is determined by the specific ionic and hydrophobic interactions. Note that reactions 2a and 3a represent the self-decay process, which competes with electron injection (reactions 2b and 3b). The distribution of distances between the dye molecules and the TiO<sub>2</sub> surface affects the rates of electron injection. The self-decay of the excited dyes, such as observed in a Nafion layer in the absence of TiO<sub>2</sub>,<sup>46c</sup> also obeys a multiexponential rate law that has been attributed to different interactions of the hydrophobic and ionic segments.<sup>46b</sup>

Control experiments in TiO<sub>2</sub> free layers were carried out only for Nafion, since SDS and SDBS do not form appropriate layers. The slow and the fast rates are 1.6 and 2 times, respectively,

faster when  $\text{TiO}_2$  is present, indicating that electron injection takes place concurrently with self-decay to the ground state. Indeed, bleaching experiments (will be presented in the following) confirm that electron injection competes with self-decay in all these systems. Note that self-decay and electron injection are kinetically indistinguishable when only emission is measured. The reaction rate constants are reported here in terms of the apparent rate constants (2) and (3). Rate constants for electron injection can be derived with the aid of the quantum yields for the specific electron injection reactions.



Reaction rate constants were derived with the aid of a simulation program for multireaction kinetics (generously provided by H. A. Schwarz of BNL). Typical experimental and the respective computed traces are shown for the dry (Figure 1s) and wet (Figure 2)  $\text{TiO}_2$ -SDBS- $\text{Ru}(\text{bpy})_3^{2+}$  systems. All the systems that were investigated behave similarly.

The solid curves in Figures 1s and 2 were computed on the basis of reactions 1–6 to give best fits with the experimental time profiles. The same rate constants fit emission data obtained in a wide range of laser light intensities (differing by up 2 orders of magnitude) and the detailed time profiles showing decay of >99% of the initial emission intensities. The fact that the same kinetic parameters are obtained in a wide range of laser beam intensities (varied within a factor of 100) strongly supports the proposed occurrence of both first- and second-order processes. Reaction 6 usually amounts to only <2% of the emission and was invoked in order to obtain a precise fit at the longer time range. The strong variation of the relative contributions of reactions 2–5 with pulse intensity and time and the fact that the fast and slow processes are reasonably well separated in time add to the reliability of the resulting constants. Thus, at the lowest intensities the time profiles can be fitted with two first-order rate constants, differing by a factor of 10. These rate constants have been used at the higher intensities at which the second-order constants have been determined.

The need to include bimolecular triplet–triplet annihilation is obvious when one compares the relative lifetimes as a function of laser pulse intensities (intensities increase from a to e in Figure 1s and from a to e in Figure 2). Even qualitative examination of the results at various intensities clearly shows shortening of lifetimes as the intensities are increased. If only first-order processes were important, the lifetimes would have remained constant, clearly in contrast with both Figures 1s and 2.

The comparison of experimental and computed initial concentrations of excited dyes and values of reaction rate constants giving best fits are summarized in Tables 1 and 1s–4s. Average computed rate constants and relative yields are presented in Table 5. The effect of added iodide ions (0.1–0.25 M) is summarized in Table 6.

In calculating the concentrations and second-order rate constants we assumed identical emission quantum yields of the excited dye molecules involved in reactions 4 and 5. In reality, different contributions of the hydrophobic and ionic bindings exerted by the polymer and the surfactants may affect the emission yields. The specific yields and bimolecular rate constants reported in this article may have to be modified if reliable information concerning these environmental effects

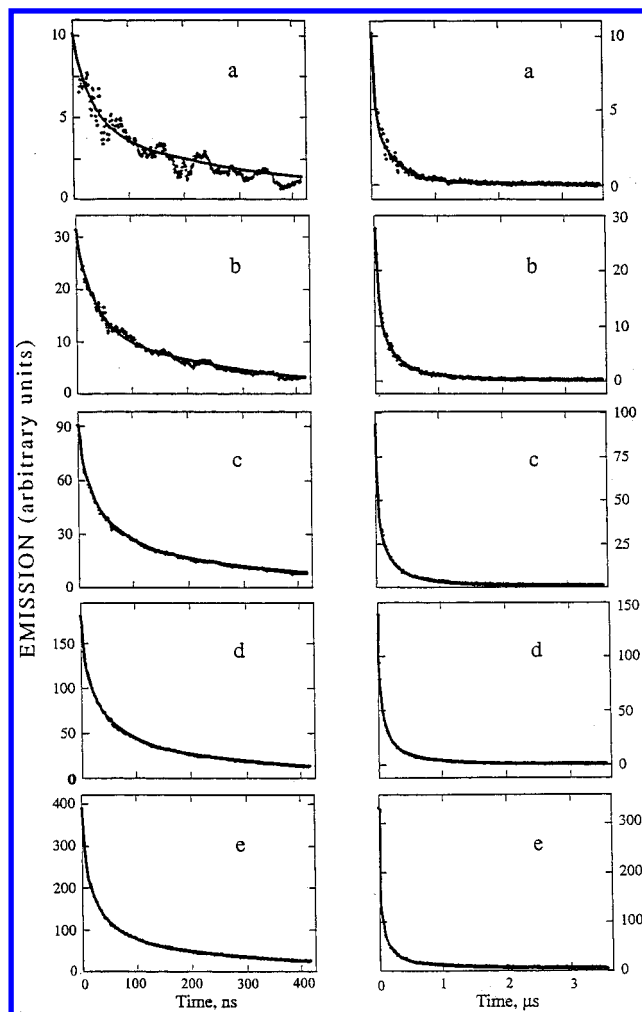


**Figure 2.** Decay of emission in the wet  $\text{TiO}_2$ /SDBS/ $\text{Ru}(\text{bpy})_3^{2+}$  system. Curves computed on the basis of reactions 1–5, using  $k_2 = 1.8 \times 10^6$ ,  $k_3 = 1.9 \times 10^7 \text{ s}^{-1}$ ,  $k_4 = 1.4 \times 10^{14}$ , and  $k_5 = 6.0 \times 10^{15} \text{ mol}^{-1} \text{ cm}^2 \text{ s}^{-1}$ . Reaction 6 was neglected. Curves a–e represent five different laser pulse intensities (see Table 2s for intensity and for initial (computed)  $(*\text{Ru}(\text{bpy})_3^{2+})_s$ ,  $(*\text{Ru}(\text{bpy})_3^{2+})_f$ , and  $(*\text{Ru}(\text{bpy})_3^{2+})_{st}$  concentrations).

become available. However, since the proportionality factor between the initial emission intensity and the measured total initial concentration of the excited states is the same, within a factor of  $\sim 2$  in all systems, we believe that the second-order rate constants are correct within a factor of better than 2.

**Discussion of the Multiexponential Emission Decay.** A multiexponential decay of excited  $\text{Ru}(\text{bpy})_3^{2+}$  and related compounds is known to occur both in thin polymer layers in the absence of semiconductors and at semiconductor surfaces in the absence of polymer and surfactant binders. Thus, Kaneko and his co-workers have recently reported three-exponential decays of  $*\text{Ru}(\text{bpy})_3^{2+}$  in Nafion layers and attributed the multiexponential decay to distribution of the dye in regions of different hydrophobicities.<sup>47</sup> Emission profiles in metal oxide powders,<sup>49–51</sup> layers,<sup>10,52</sup> and sols,<sup>12,48,53</sup> involving  $\text{Ru}(\text{bpy})_3^{2+}$ ,  $\text{Ru}(\text{bpy})_2(\text{dcbpy})^{2+}$  (dcbpy stands for 4,4'-dicarboxy-2,2'-bipyridine),  $\text{Ru}(\text{dcbpy})_2\text{X}_2$  ( $\text{X}^- = \text{Cl}^-$ ,  $\text{CN}^-$ ,  $\text{SCN}^-$ ), and other dyes adsorbed to various metal oxides have been recently reported. In these systems, the predominant reaction is electron injection from the excited state to the semiconductor, although it is usually restricted to low surface coverage.

Very fast rates of electron injections from excited singlet states take place with lifetimes on the order of  $< 10 \text{ ps}$ <sup>50,54</sup> at dye coverage of less than 0.01, when the excited vibronic state is by  $> 0.5 \text{ eV}$  above the edge of the conduction band of the semiconductor particle. At higher coverage, aggregates of dye

**TABLE 1: TiO<sub>2</sub>–SDS–Ru(bpy)<sub>3</sub><sup>2+</sup> System: Experimental and Computed Yields and Rate Constants; 70% of the Laser Light Was Initially Absorbed by the Ru(bpy)<sub>3</sub><sup>2+</sup>; Supporting Information for Ru(o-phen)<sub>3</sub><sup>2+</sup> in Table 1s**

experimental conditions		computed parameters giving best fits							
		$\times 10^{10}$ mol/cm <sup>2</sup>			$\times 10^6$ s <sup>-1</sup>			$\times 10^{14}$ mol <sup>-1</sup> cm <sup>2</sup> s <sup>-1</sup>	
		Ru(bpy) <sub>3</sub> <sup>2+</sup> <sub>s</sub>	Ru(bpy) <sub>3</sub> <sup>2+</sup> <sub>f</sub>	Ru(bpy) <sub>3</sub> <sup>2+</sup> <sub>st</sub>	k <sub>2</sub>	k <sub>3</sub>	k <sub>6</sub>	k <sub>4</sub>	k <sub>5</sub>
intensity <sup>a</sup> $\times 10^{10}$	time ns/div <sup>b</sup>								
2.6 D	50	0.8	1.8	0	2.2	12		2.8	28
10.5 D	50–200	3.5	6.4	0	2.3	14		2.8	28
42 D	50–200	10.4	18.2	0	2.4	15		3.5	30
124 D	50	22.9	37.8	0	2.3	13		2.9	29
320 D	50–200	50.4	91.6	0	2.2	13		3.1	23
2.5 W	50–200	1.5	1.0	0	1.7	24		1.9	55
10.4 W	20–200	5.1	4.7	0–0.14	1.7	24	0.4	1.7	55
41 W	50–200	15.5	13.6	0	1.8	20		3.0	70
120 W	50–200	35	31	0–2.7	1.8	20	0.4	2.8	90
310 W	20–200	78	73	0–3.6	2	20	0.4	1.7	60

<sup>a</sup> Absorbed einsteins per cm<sup>2</sup>. Uncorrected for bleaching during laser pulse. <sup>b</sup> Total time of measurement corresponds to nine divisions. D = dry layers; W = wet layers.

**TABLE 5: Summary of Rate Constants**

system	slow (%) <sup>a</sup>	fast (%) <sup>a</sup>	ST (%) <sup>a</sup>	× 10 <sup>-6</sup> s <sup>-1</sup>			× 10 <sup>-14</sup> mol <sup>-1</sup> cm <sup>2</sup> s <sup>-1</sup>	
				k <sub>2</sub>	k <sub>3</sub>	k <sub>6</sub>	k <sub>4</sub>	k <sub>5</sub>
TiO <sub>2</sub> /SDS/Ru(bpy) <sub>3</sub> <sup>2+</sup> , dry	35	65	0	2.3	14		3.0	26
TiO <sub>2</sub> /SDS/Ru(bpy) <sub>3</sub> <sup>2+</sup> , wet	52	45	3	1.7	24	0.4	2.4	76
TiO <sub>2</sub> /SDBS/Ru(bpy) <sub>3</sub> <sup>2+</sup> , dry	43	55	2	3.0	28	0.5	16	110
TiO <sub>2</sub> /SDBS/Ru(bpy) <sub>3</sub> <sup>2+</sup> , wet	35	65	0	1.8	19		1.4	60
TiO <sub>2</sub> /Nafion/Ru(bpy) <sub>3</sub> <sup>2+</sup> , dry	33	67	0	3.0	19		1.5	17
Nafion/Ru(bpy) <sub>3</sub> <sup>2+</sup> , dry	41	59	0	1.3	13		9.5	125
TiO <sub>2</sub> /Nafion/Ru(bpy) <sub>3</sub> <sup>2+</sup> , wet	52	48	0	1.9	13		3.0	35
Nafion/Ru(bpy) <sub>3</sub> <sup>2+</sup> , wet	43	57	1	1.1	9		2.9	48
TiO <sub>2</sub> /SDS/Ru(o-phen) <sub>3</sub> <sup>2+</sup> , dry	45	54	1	1.1	12		1.4	21
TiO <sub>2</sub> /SDS/Ru(o-phen) <sub>3</sub> <sup>2+</sup> , wet	68	31	1	0.8	13		1.15	16
TiO <sub>2</sub> /SDBS/Ru(o-phen) <sub>3</sub> <sup>2+</sup> –dry	31	64	5	2.4	21	0.3	2.9	60
TiO <sub>2</sub> /SDBS/Ru(o-phen) <sub>3</sub> <sup>2+</sup> –wet	43	56	1	2.0	20	0.2	5.5	80
TiO <sub>2</sub> /Naf/Ru(o-phen) <sub>3</sub> <sup>2+</sup> , dry	33	65	2	3.2	25			
Naf/Ru(o-phen) <sub>3</sub> <sup>2+</sup> , dry	42	56	2	1.9	14		10	125
TiO <sub>2</sub> /Naf/Ru(o-phen) <sub>3</sub> <sup>2+</sup> , wet	49	51	0	2.7	18			
Naf/Ru(o-phen) <sub>3</sub> <sup>2+</sup> , wet	43	56	1	1.2	11		6.6	77

<sup>a</sup> “slow”, “fast” and “ST” stand for the processes described by reactions 2 and 4, 3 and 5, and 6, respectively.

**TABLE 6: Reaction Rate Constants and Quantum Yields in the TiO<sub>2</sub>/X/Ru(bpy)<sub>3</sub><sup>2+</sup> System<sup>a</sup>**

system	absorbed light (einsteins/cm <sup>2</sup> × 10 <sup>10</sup> )	k <sub>7f</sub> (s <sup>-1</sup> )	k <sub>7s</sub> (s <sup>-1</sup> )	φ(f)	φ(s)	φ(r)
X ≡ SDS, dry	24.5	6 × 10 <sup>5</sup>	9.0 × 10 <sup>4</sup>	0.27 (0.38)	0.34 (0.47)	0.02
X ≡ SDS, dry	90–110	6 × 10 <sup>5</sup>	7.5 × 10 <sup>4</sup>	0.14 (0.38)	0.07 (0.19)	0.03
X ≡ SDS, dry	190–230	9 × 10 <sup>5</sup>	8.0 × 10 <sup>4</sup>	0.15 (0.50)	0.11 (0.45)	0–0.03
average		7.0 × 10 <sup>5</sup>	8.2 × 10 <sup>4</sup>	0.42 ± 0.12	0.38 ± 0.12	0.03
X ≡ SDS, wet	26	8.0 × 10 <sup>5</sup>	7.6 × 10 <sup>4</sup>	0.23 (0.29)	0.33 (0.47)	0.01
X ≡ SDS, wet	47		7.5 × 10 <sup>4</sup>		0.20 (0.30)	0.015
X ≡ SDS, wet	90–96	9.0 × 10 <sup>5</sup>	8.5 × 10 <sup>4</sup>	0.11 (0.27)	0.19 (0.45)	0.015
X ≡ SDS, wet	190–210	6.3 × 10 <sup>5</sup>	6.6 × 10 <sup>4</sup>	0.08 (0.22)	0.13 (0.61)	0–0.03
average		7.5 × 10 <sup>5</sup>	7.5 × 10 <sup>4</sup>	0.26 ± 0.07	0.46 ± 0.12	0.01
X ≡ SDBS, dry	120	2.5 × 10 <sup>5</sup>	1.0 × 10 <sup>4</sup>	0.044 (0.25)	0.045 (0.25)	0.01
X ≡ SDBS, dry	270	2.5 × 10 <sup>5</sup>	1.2 × 10 <sup>4</sup>	0.040 (0.36)	0.046 (0.42)	0–0.02
average		2.5 × 10 <sup>5</sup>	1.1 × 10 <sup>4</sup>	0.31 ± 0.05	0.33 ± 0.08	0–0.02
X ≡ SDBS, wet	110	2.5 × 10 <sup>5</sup>		0.095 (0.18)	0.051 (0.21)	0–0.01
X ≡ SDBS, wet	240	2.3 × 10 <sup>5</sup>	3.0 × 10 <sup>3</sup>	0.062 (0.14)	0.054 (0.27)	0.01
average		2.4 × 10 <sup>5</sup>	3.5 × 10 <sup>3</sup>	0.16 ± 0.05	0.24 ± 0.07	0.01

<sup>a</sup> The signs “f”, “s”, and “r” denote the fast and the slow recovery of the ground state, and the residual bleaching, respectively. Ground state absorbance at 460 nm was 0.5. Bleaching was measured at 420 nm. Quantum yields were calculated using Δε(Ru(bpy)<sub>3</sub><sup>2+</sup> – Ru(bpy)<sub>3</sub><sup>3+</sup>) = 8.2 × 10<sup>6</sup> mol<sup>-1</sup> cm<sup>2</sup>.<sup>64</sup> Most values in the table represent averages of 2–3 time profiles. The φ values in parentheses are corrected for both the observed triplet–triplet annihilation of the excited \*Ru(bpy)<sub>3</sub><sup>2+</sup> and the nonlinearity of the initial triplet signal with respect to absorbed light intensity (discussed in the emission sections). Statistical error margin for single rate constants was 10–20%. Supporting Information (the Nafion system) is available in Table 6s.

molecules act as fast traps (electron sinks) competing with electron injection to the semiconductor.<sup>55</sup>

Emission from triplets decays at semiconductor surfaces in the nanosecond time range, considerably slower than singlets but much faster than in the present work. As a matter of rule, emission vs time profiles in the absence of binders such as SDS, SDBS, and Nafion show also several exponential decays. These have been attributed to the existence of adsorption sites differing

in energy levels.<sup>49</sup> Thus, Ru(bpy)<sub>3</sub><sup>2+</sup> or Ru(bpz)<sub>3</sub><sup>2+</sup> ions adsorbed to SnO<sub>2</sub>, TiO<sub>2</sub> or SrTiO<sub>3</sub> (vacuum) show four-exponential decays,<sup>49b</sup> respectively, with rate constants changing by up to a factor of 500 in a given system. Nafion, in the absence of TiO<sub>2</sub> shows three-exponential decays. In the present work, the simultaneous interactions between the dye molecules, TiO<sub>2</sub>, and Nafion control the rates, and the original TiO<sub>2</sub> sites with different energy levels are not relevant in the presence of

a binder. The observed slower reaction rates are attributed to the increased average distance between the photosensitizer and TiO<sub>2</sub> surface because of the presence of binders, producing a new broad distribution of rates that fits the two observed lifetimes.<sup>46b</sup> This will be further discussed later.

In contrast with the relatively mild effect of water on the rates of emission decay in this work, adsorbed water slows the fastest luminescence decay in binder-free Ru(bpy)<sub>3</sub><sup>2+</sup>/TiO<sub>2</sub><sup>49a</sup> by an order of magnitude, without affecting as much the slower decays. This has been attributed to weakening of the interaction of the Ru complex with the TiO<sub>2</sub> by the adsorbed water. In our systems, however, this effect is minimized because of two reasons. Firstly, as will be seen later, yields of electron injection for most systems range between 30% and 80% (Ru(o-phen)<sub>3</sub><sup>2+</sup> in dry SDBS and in dry Nafion have lower yields). When self-decay is predominant, rates are not expected to change much upon weakening of the interactions between the dyes and TiO<sub>2</sub>. Secondly, since in the present work the photosensitizers are adsorbed to the TiO<sub>2</sub> by means of their interactions with the binders, the negative ionic charges of the binders together with the hydrophobic interactions (helping to bind the photosensitizers and repel water molecules) more than compensate for the electrostatic repulsion between the TiO<sub>2</sub> surface and photosensitizer ions. Consequently, the effect of water on the rate of electron injection is much smaller than in the absence of binders.

**The First-Order Rates and Average Distance from the TiO<sub>2</sub> Surface.** The first order reaction rate constants in the present work,  $2 \times 10^7$  and  $2 \times 10^6$  s<sup>-1</sup> for the fast and slow decays, respectively, are much slower than similar decay rates in the absence of binders. Thus, emission decay rates (attributed to electron injection) from \*Ru(bpy)<sub>3</sub><sup>2+</sup> triplet to TiO<sub>2</sub>, SnO<sub>2</sub>, or ZnO are 10–50 times faster,<sup>49a,b</sup> and from \*Ru(dcbpy)-(bpy)<sub>2</sub><sup>2+</sup> triplet to TiO<sub>2</sub>, SnO<sub>2</sub>, or ZnO are 5–20 times faster than here.<sup>51,52</sup> Electron injection from Ru(bpy)<sub>3</sub><sup>2+</sup> electrostatically adsorbed to SnO<sub>2</sub> sol is completed within 50 ns,<sup>53</sup> much faster than in our systems. The rate of electron injection is affected by the average distance of the excited electron from the surface. Direct linkage of a Ru(II) complex to the surface favors fast electron transfer. Separation by water such as in ref 49a or by the organic groups used to bind the photosensitizer to the surface decreases the rate. The dcbpy complexes form an ester linkage with the semiconductor hydroxyl groups.<sup>10</sup> Since the triplet states in the Ru–bipyridine derivatives are produced by MLCT, electron injection takes place from a very near distance as the photosensitizer is separated from the surface merely by a CO group. This explains the high injection rates observed for \*Ru(dcbpy)<sub>2</sub>X<sub>2</sub><sup>2+</sup> ( $k > 5 \times 10^7$  s<sup>-1</sup>)<sup>10</sup> and Ru(dcbpy)(bpy)<sub>2</sub><sup>2+</sup> ( $k = (1-5) \times 10^8$ )<sup>50,52</sup>.

The relatively slow rates of decay of emission in our systems compared with direct adsorption of the dyes can be related to the properties of the binders and their interactions with the photosensitizers. Ru(bpy)<sub>3</sub><sup>2+</sup> is known to form strong hydrophobic<sup>56</sup> as well as ionic bindings. Ru(o-phen)<sub>3</sub><sup>2+</sup> is even more hydrophobic than Ru(bpy)<sub>3</sub><sup>2+</sup>. Both SDS and SDBS are expected to produce ion pairs of the type Ru(II)(Surfactant)<sub>2</sub>,<sup>57</sup> so that the effective distance between the excited dye molecules and the TiO<sub>2</sub> surface is larger than in Ru(II) complexes which are directly adsorbed. Separation between the surface by a hydrophobic segment of a surfactant molecule may induce further decrease of the electron injection rates. The situation in the Nafion systems is somewhat different, since the Nafion forms a very thin layer on the TiO<sub>2</sub> surface, into which the photosensitizer molecules penetrate. The electrostatic and hydrophobic interactions of the dyes with the Nafion increase their average distance from the surface. Note that adsorption of Nafion takes place by the combined electrostatic and

hydrophobic interactions with the TiO<sub>2</sub>. The importance of the electrostatic forces is evident from the fact that no observable uptake of Nafion (as well as SDS or SDBS) occurs at neutral pH, where the Nafion is negatively charged while the TiO<sub>2</sub> is near its point of zero charge. Hydrophobic bindings are expected to induce some separation between the TiO<sub>2</sub> surface and the dyes by hydrophobic segments of the Nafion. In this context it is interesting to note that once Nafion or SDBS is adsorbed to the TiO<sub>2</sub> surface and is loaded with the dyes, increasing the pH to the zero charge point does not remove the binders. This demonstrates the importance of the interactions between the TiO<sub>2</sub> and the hydrophobic groups of the binders.

Our results are in agreement with recent electron injection studies by Ford and Rodgers.<sup>53</sup> In their study, electron injection rates from \*RuL<sub>3</sub><sup>2+</sup> covalently linked to the semiconductor (SnO<sub>2</sub>) nanocrystallite by a chain containing 11 bonds were compared to a similar Ru complex directly adsorbed by electrostatic bindings. Although the covalently linked photosensitizer was not rigidly held at a distance, the separation caused a remarkable decrease in the rate of electron injection. Although no sufficient data are given for quantitative comparison of the emission decays, comparison between Figures 1s and 2 (this work) to Figure 5 (ref 53) show close similarity. Note that in the present work,  $\Delta G^\circ$  for electron injection is -0.45 eV ( $E^\circ(3+/2+)$  for \*Ru(bpy)<sub>3</sub><sup>2+</sup> is -0.85 and  $E_{cb}$  for TiO<sub>2</sub> at pH 2.5 = -0.4 V vs NHE), which is comparable to the respective value (-0.5 eV) in the RuL<sub>3</sub><sup>2+</sup>/SnO<sub>2</sub> system at pH = 4 ( $E_{cb}$  = -0.34 V for SnO<sub>2</sub> at pH 4).

**Bleaching Kinetics and Yields.** Time profiles of bleaching at 420 nm (excitation at 460 nm) were recorded in the range up to 150 μs, using laser beam intensities ranging from  $3.8 \times 10^{-10}$  to  $4.6 \times 10^{-8}$  einsteins/cm<sup>2</sup> per pulse. TiO<sub>2</sub> layers loaded with Ru(bpy)<sub>3</sub><sup>2+</sup> or Ru(o-phen)<sub>3</sub><sup>2+</sup>, after treatment with SDS, SDBS, or Nafion, were investigated in the dry and wet states. Note that the following reaction sequence is given for Ru(bpy)<sub>3</sub><sup>2+</sup>, although Ru(o-phen)<sub>3</sub><sup>2+</sup> behaves similarly. Bleaching of the absorbance occurs during the laser pulse and is followed by three absorbance formation steps, at the end of which the ground state spectrum is fully regenerated: a relatively fast process that takes place in the time range where the decay of emission is observed. Although quantitative measurement of this process is not possible (the time resolution with the 500 Ω termination was 100 ns), this process undoubtedly represents predominantly reactions (3) and (5) with some contribution of reactions 2 and 4. Electron injection from the Ru(II) excited state to the TiO<sub>2</sub> (reactions 2b and 3b) is expected to produce additional bleaching at 420 nm, but the competing reactions (2a, 3a, 4, and 5) all contribute to a buildup of absorbance. The extinction coefficients of Ru(II), Ru(II)\*, and Ru(III) are such that 20% of the Ru(II)\* decaying without electron injection is enough to compensate for the bleaching that results from electron injection. Since the quantum yields for electron injection are usually considerably less than unity (note that bleaching could be measured only at the relatively high laser pulse intensities where the bimolecular reactions 4 and 5 are important), the above fast recovery of bleaching is not surprising.

In nearly all systems, a biexponential regeneration of the ground state absorbance (reaction 7) follows the fast process in the time range 1–150 μs. The two first-order reaction rate constants used to fit the time profiles depend on the specific system involved. Again, the biexponential nature of reaction 7 is attributed to the distribution of binding interactions (electrostatic and hydrophobic) and, related to this, distances between the reacting species. Typical bleaching profiles are presented in Figures 3s and 4. Note that although eq 7 represents a bimolecular process, while  $k_{7s}$  and  $k_{7f}$  are computed

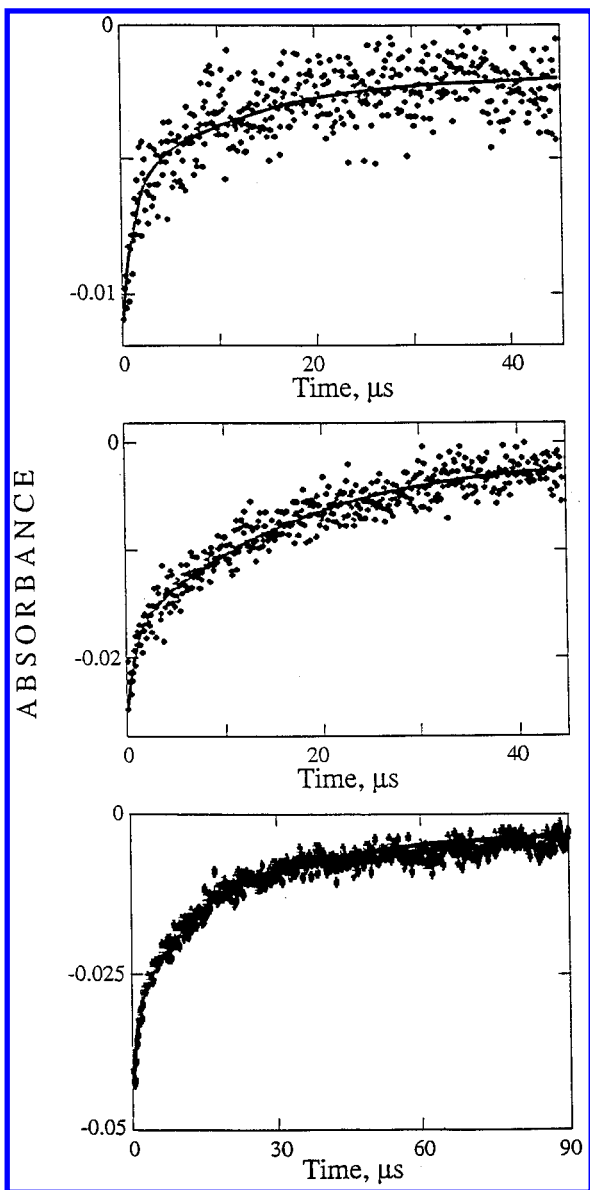
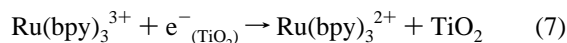


**Figure 4.** Bleaching profiles for TiO<sub>2</sub>/SDS/Ru(bpy)<sub>3</sub><sup>2+</sup> wet system. (a) Absorbed light  $2.5 \times 10^{-9}$  einsteins/cm<sup>2</sup> per pulse. Solid line: best fit yielding  $\phi_s = 0.33$ ,  $\phi_f = 0.23$ ,  $\phi_r = 0.01$ ,  $k_{7s} = 7.6 \times 10^4$ , and  $k_{7f} = 8 \times 10^5$  s<sup>-1</sup>. (b) Absorbed light  $9.6 \times 10^{-9}$  einsteins/cm<sup>2</sup> per pulse. Solid line: best fit yielding  $\phi_s = 0.22$ ,  $\phi_f = 0.21$ ,  $\phi_r = 0.01$ ,  $k_{7s} = 8.7 \times 10^4$ , and  $k_{7f} = 8.4 \times 10^5$  s<sup>-1</sup>. (c) Absorbed light  $2.1 \times 10^{-8}$  einsteins/cm<sup>2</sup> per pulse. Solid line: best fit yielding  $\phi_s = 0.15$ ,  $\phi_f = 0.20$ ,  $\phi_r = 0.02$ ,  $k_{7s} = 6.1 \times 10^4$ , and  $k_{7f} = 6.6 \times 10^5$  s<sup>-1</sup>.

from exponential fits, the resulting values are independent of laser pulse intensity. This is expected if each pair of Ru(bpy)<sub>3</sub><sup>3+</sup> and e<sup>-</sup>(TiO<sub>2</sub>) reacts independently of the others, in which case changing the laser pulse intensity results in a variation of the number of independently reacting pairs. This leaves the lifetime unchanged, as observed. On the other hand, if each of the reactants is capable of reacting with a number of partners, the lifetime is expected to become shortened as the intensity is increased, which is contrary to the observation. We conclude that process 7 represents the back reaction of trapped electrons with their parent Ru compound.



Electron injection from the excited photosensitizer to TiO<sub>2</sub> (reactions 2b, 3b) and electron recapture by the Ru(III) complex (reaction 7) are evident from comparison of the lifetimes of bleaching and emission. Typical examples are shown in Figure

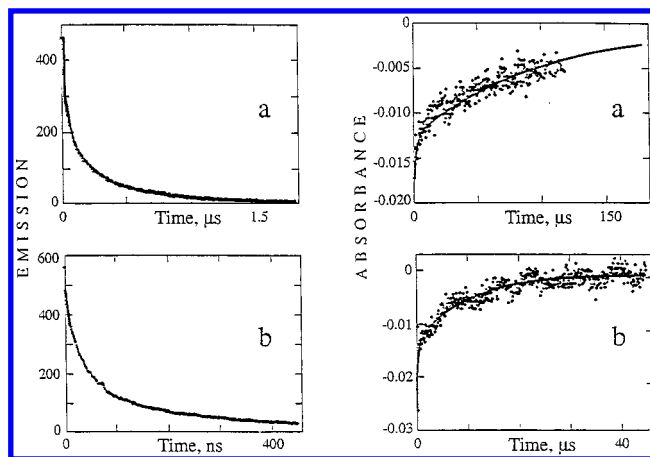


**Figure 5.** Comparison of bleaching with emission profiles. (a) TiO<sub>2</sub>/Nafion/Ru(bpy)<sub>3</sub><sup>2+</sup> wet system. Absorbed light  $2.0 \times 10^{-8}$  einsteins/cm<sup>2</sup> per pulse. Solid lines: bleaching fitted with  $\phi_s = 0.075$ ,  $\phi_f = 0.033$ ,  $\phi_r = 0$ ,  $k_{7s} = 1.0 \times 10^4$ , and  $k_{7f} = 5.7 \times 10^5$  s<sup>-1</sup>. Emission is shown on an arbitrary scale. (b) TiO<sub>2</sub>/Nafion/Ru(bpy)<sub>3</sub><sup>2+</sup> dry system. Absorbed light  $2.1 \times 10^{-8}$  einsteins/cm<sup>2</sup> per pulse. Solid lines: bleaching fitted with  $\phi_s = 0.074$ ,  $\phi_f = 0.010$ ,  $\phi_r = 0$ ,  $k_{7s} = 1.03 \times 10^5$ , and  $k_{7f} = 5 \times 10^6$  s<sup>-1</sup>. Emission is shown on an arbitrary scale.

5, where bleaching and emission time profiles are compared in the TiO<sub>2</sub>/Nafion/Ru(bpy)<sub>3</sub><sup>2+</sup> dry and wet systems, respectively. The emission traces were taken using a termination of 50 Ω, while the bleaching was measured using a 500 Ω termination (response time 30 ns). Figure 5 shows that the emission decays much faster than the rate of recovery of the ground state absorption. This feature has been found to be typical of other systems as well, although in some cases (will be discussed later), reactions 2 and 7f are not well separated in time. Bleaching takes place during the laser pulse because \*Ru(bpy)<sub>3</sub><sup>2+</sup> has much smaller absorbance compared to the ground state.

Blank experiments, namely, bleaching measurements in the absence of TiO<sub>2</sub>, are possible only in the case of Nafion, because the two surfactants, SDS and SDBS, are not known to produce transparent layers. Comparison between the time profiles in the absence and in the presence of TiO<sub>2</sub> (Figure 6) clearly demonstrates longer bleaching lifetimes in the presence of TiO<sub>2</sub>. In the absence of binders only negligible bleaching can be observed, because there is practically no adsorption of the dyes at pH 2.5 in the absence of binders.

The quantum yields for electron injection were calculated on the basis of actinometry with a Ru(bpy)<sub>3</sub><sup>2+</sup> solution, measuring the initial bleaching of the actinometer. The separate quantum yields for the fast and slow steps, respectively, were determined by curve fittings, based on the mechanism presented above. The fast and slow steps are reasonably well separated in time.

Tables 6 and 7s contain the detailed results for Ru(bpy)<sub>3</sub><sup>3+</sup> and Ru(o-phen)<sub>3</sub><sup>3+</sup>, respectively. A summary of these results is presented in Table 8. The measurements were carried out in Ar atmosphere at pH 2.5 (HClO<sub>4</sub>). The computed reaction rate constants,  $k_{7(\text{fast})}$  and  $k_{7(\text{slow})}$ , are independent of laser pulse intensity, in agreement with the first-order nature of reactions 7. The residual absorbance that is observed in some of the systems (usually corresponding to quantum yield < 0.015) is too small for detailed investigations. Note that analytical light instability may cause apparent residual bleaching or absorbance, but such an effect is expected to give random fluctuations rather than systematic residual bleaching.

The quantum yields of bleaching have been calculated by extrapolation of the computed time profiles to the end of the laser pulse. This procedure minimizes errors which may be introduced upon direct measurements of the initial bleaching when reaction (2) is not completely separated in time from the



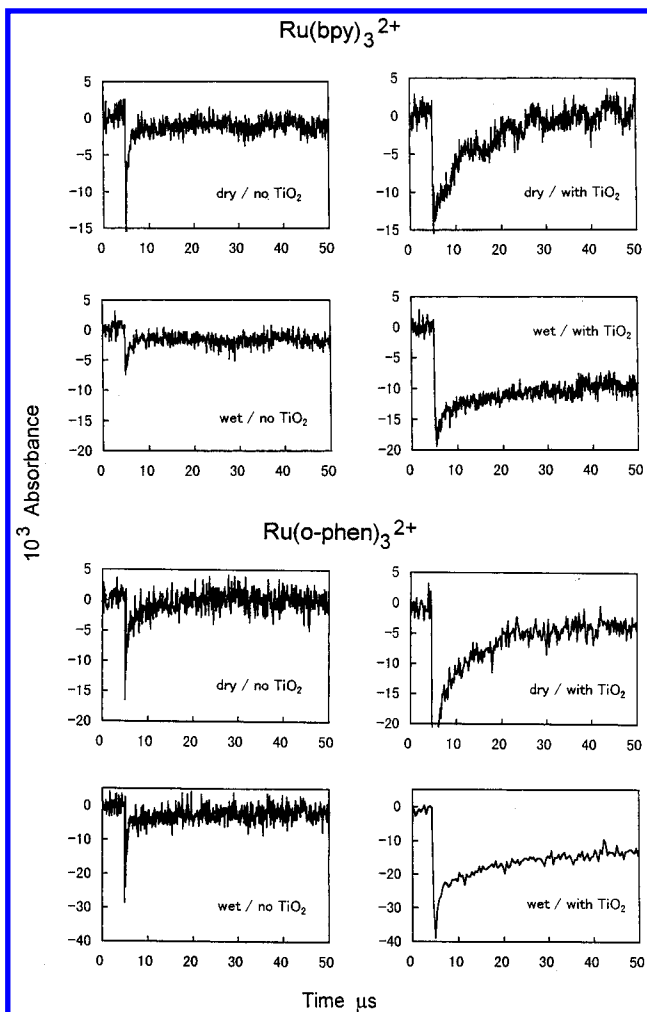


**Figure 6.** Comparison of bleaching profiles in Nafion and Nafion/TiO<sub>2</sub> layers. The curves on the left-hand side represent bleaching at 460 nm in TiO<sub>2</sub>-free Nafion layers. Curves on the right-hand side represent bleaching in TiO<sub>2</sub>-Nafion layer systems. Absorbed laser light  $(2.0 \text{ and } 2.6) \times 10^{-8}$  einsteins/cm<sup>2</sup> per pulse for Ru(bpy)<sub>3</sub><sup>2+</sup> and Ru(o-phen)<sub>3</sub><sup>2+</sup>, respectively.

faster component of reaction 7. Despite this precaution, some error is likely to occur in the dry TiO<sub>2</sub>/Nafion/Ru(bpy)<sub>3</sub><sup>2+</sup> and in wet TiO<sub>2</sub>/SDS/Ru(o-phen)<sub>3</sub><sup>2+</sup>, which have the poorest time separation. Figure 6 shows that even for the dry Nafion/Ru(bpy)<sub>3</sub><sup>2+</sup> system, TiO<sub>2</sub> has a remarkable effect on the bleaching lifetime, unequivocally demonstrating the importance of electron injection.

The quantum yields calculated by extrapolation of the kinetic traces are affected by the triplet-triplet annihilation, the contribution of the latter depending on laser pulse intensity. Another factor affecting the quantum yields is the fast annihilation of triplets during the laser pulse, which we attribute to very rapid energy migration at high laser pulse intensities. When steady state illumination is applied, such as used for photocurrent generation, triplet-triplet annihilation is negligible. Quantum yields were corrected for the high-intensity effects by using the contribution of the first-order reactions only. This was carried out with the aid of computer simulations for the time profiles of each reactant and product, using the reaction rate constants determined from the respective emission profiles. Corrections include adjustment of the absorbed excitation light to exclude the fraction of excited states that decay during the laser pulse. This fraction highly depends on the laser intensity and does not contribute to the first-order electron injection. It is not observed at very low intensities, but the bleaching experiments required the use of relatively high intensities in order to obtain

sufficiently high signals. The corrected quantum yields are given in Tables 7s and 8 in parentheses. Note that in all systems rates of decay of bleaching are much slower than the corresponding rates of decay of emission. With the exception of the two systems mentioned above, the time separation between reaction 2 and 7 is enough to provide reasonably accurate values of  $\varphi_f$  from the computed initial bleaching values. In all the systems values of  $\varphi_s$  can be directly measured because the slower component of reaction 7 is always well separated in time from reaction 2.

**The Apparent First-Order Nature of Recombination Kinetics: Comparison with Band Gap Excitation.** The TiO<sub>2</sub> membrane layer used in this work is composed of nanocrystallites with average diameter about 10 nm.<sup>6</sup> The magnitude of the initial measurable bleaching corresponds to 0.5–5 Ru(III)–electron pairs per nanocrystallite. Reactions 7s in the various systems involve an average of 0.8–1.6 pairs per nanocrystallite. Since both reactions 7s and 7f obey a first-order rate law, one must conclude that each electron reacts with its parent Ru(III) ion. This interpretation is in agreement with the conclusions of Martin, Herrmann, and Hoffmann,<sup>30,31</sup> based on time-resolved microwave conductivity studies in band gap excited TiO<sub>2</sub> colloid solutions. Band gap excitation produces mobile electrons and holes that undergo very rapid recombination in competition with surface trapping, in the time range of pico- to nanoseconds.<sup>58</sup> When the residual concentration of carriers drops below a critical level ( $\sim 10^{18}$  cm<sup>-3</sup> in TiO<sub>2</sub> Q-particles<sup>31</sup>), recombination becomes relatively slow ( $\tau$  in the micro- and millisecond time ranges<sup>30,31</sup>). In the present work, surface holes, in the form of adsorbed Ru(III), are formed by the electron injection process. The redox potentials of the excited dyes are sufficiently negative and enable electron injection to the conduction band ( $\epsilon^\circ$  is  $-0.84$  and  $-0.87$  for excited Ru(bpy)<sub>3</sub><sup>2+</sup> and Ru(o-phen)<sub>3</sub><sup>2+</sup>, respectively,<sup>59</sup> compared with  $-0.5$  V for the Q-TiO<sub>2</sub><sup>60</sup>). However, comparison of the recombination kinetics observed in this work to that measured upon direct band gap excitation<sup>30,31</sup> suggests that there is a sufficient number of low-energy states available to accept the injected electrons near the parent molecules. Since the electrons become trapped near the parent photosensitizer molecule, the back reaction involves independently reacting pairs. This explains not only the first-order rate law obeyed by the recombination, but also the faster rate of reaction compared to the direct band gap excitation. In the latter case, a substantial fraction of the electron–hole pairs have a lifetime in the millisecond time range. Such slow back reactions are observed also in the presence of a surface hole scavenger, such as Cl<sup>-</sup> ions, which are very quickly oxidized by mobile holes and form adsorbed Cl atoms. The different space distributions result from the different nature of the electron and hole precursors: direct band gap excitation produces mobile holes and electrons, respectively, and trapping occurs in sites randomly distributed on the entire nanocrystallite surface. On the other hand, as discussed above, electron injection under our conditions results in trapped electron–hole pairs at close proximity. Consequently, the average electron–hole distances produced by band gap excitation are larger than between pairs obtained by electron injection. This induces faster recombination rates in the latter case. From the initially measurable bleaching it is possible to estimate a charge carrier density on the order of  $10^{19}$  cm<sup>-3</sup>. This is in fair agreement with the previous estimated limit for the density of low-energy electron states.<sup>31</sup>

**Effects of Different Binders on  $k_7(f)$  and  $k_7(s)$ : General.** The biexponential nature of the decay of bleaching, described in terms of reactions 7s and 7f, is attributed to distribution of lifetimes<sup>46b</sup> related to distribution of distances between the

TABLE 8: Summary of Bleaching Rates and Corrected Quantum Yields<sup>a</sup>

system	absorbed light (einsteins/cm <sup>2</sup> × 10 <sup>10</sup> )	$k_{7f}$ s <sup>-1</sup>	$k_{7s}$ s <sup>-1</sup>	$\varphi(f)$	$\varphi(s)$	$\varphi(r)$
Ru(bpy) <sub>3</sub> <sup>2+</sup>						
X ≡ SDS, dry	24.5–230	7.0 × 10 <sup>5</sup>	8.2 × 10 <sup>4</sup>	0.42 ± 0.12	0.38 ± 0.12	0.03
X ≡ SDS, wet	26–210	7.5 × 10 <sup>5</sup>	7.5 × 10 <sup>4</sup>	0.26 ± 0.07	0.46 ± 0.12	0.01
X ≡ SDBS, dry	120–270	2.5 × 10 <sup>5</sup>	1.1 × 10 <sup>4</sup>	0.31 ± 0.05	0.33 ± 0.08	0–0.02
X ≡ SDBS, wet	110–240	2.4 × 10 <sup>5</sup>	3.5 × 10 <sup>3</sup>	0.16 ± 0.05	0.24 ± 0.07	0.01
X ≡ Nafion, dry	26–210	3.5 × 10 <sup>6</sup>	1.0 × 10 <sup>5</sup>	0.16 ± 0.04	0.29 ± 0.06	0.015
X ≡ Nafion, wet	26–200	5.5 × 10 <sup>5</sup>	1.2 × 10 <sup>4</sup>	0.11 ± 0.03	0.37 ± 0.08	0.02
Ru(o-phen) <sub>3</sub> <sup>2+</sup>						
X ≡ SDS, dry	61–127	7.9 × 10 <sup>5</sup>	1.6 × 10 <sup>4</sup>	0.26 ± 0.08	0.33 ± 0.08	
X ≡ SDS, wet	17.2–127	7.7 × 10 <sup>5</sup>	6.2 × 10 <sup>4</sup>	0.19 ± 0.07	0.12 ± 0.04	
X ≡ SDBS, dry	24–190	1.1 × 10 <sup>6</sup>	3 × 10 <sup>4</sup>	0.13 ± 0.03	0.12 ± 0.03	
X ≡ SDBS, wet	86–189	6 × 10 <sup>5</sup>	6 × 10 <sup>4</sup>	0.22 ± 0.08	0.3 ± 0.1	
X ≡ Nafion, dry	117–263	9 × 10 <sup>5</sup>	5 × 10 <sup>4</sup>	0.16 ± 0.04	0.10 ± 0.03	
X ≡ Nafion, wet	31–263	5 × 10 <sup>5</sup>	1.1 × 10 <sup>4</sup>	0.17 ± 0.05	0.20 ± 0.05	

<sup>a</sup> Rate constants represent average values from the highest three intensities. Yields have been corrected for both the observed triplet–triplet annihilation and the nonlinearity of the initial triplet signal with respect to absorbed light intensity (discussed in the emission sections).

reactants. Similarly to the electron injection process, the distances between reactant molecules and the TiO<sub>2</sub> surface are related to the hydrophobic and electrostatic forces between the oxidized dyes and the binders, which are different from the respective forces involving the Ru(II) complexes because of the different ionic charges and the different hydrophobicities.

With one exception (dry Ru(bpy)<sub>3</sub><sup>3+</sup>/Nafion), the rates of reactions 7f are within a factor of 2 of the value 5 × 10<sup>5</sup> s<sup>-1</sup> in all systems. Variations in  $k_{7s}$  are larger and more difficult to generalize: up to a factor of 30 has been observed between the fastest (dry Ru(bpy)<sub>3</sub><sup>3+</sup>/Nafion) and slowest (wet Ru(bpy)<sub>3</sub><sup>3+</sup>/SDBS) rates. The much larger variations of back reaction rate constants are in contrast with the electron injection rates, which are the same, within a factor of 3, for all Ru(bpy)<sub>3</sub><sup>2+</sup> and Ru(o-phen)<sub>3</sub><sup>2+</sup> systems.

Interactions of the Ru complexes with the binders involve stabilization of Ru(II) (both ground and excited states) by hydrophobic forces and stabilization of the Ru(III) ions by electrostatic interactions. These interactions are expected to affect the driving force for both electron injection and back reactions. In addition, as a result of these interactions, each system has its specific space distribution of the Ru reactant. The similarity of the injection rates when different binders and conditions (dry and wet) are used implies that the net effects of these interactions on electron injection rates are rather small. This is in apparent contradiction with the relatively much larger variation of back reaction rates.

This can be explained in terms of the different role of the space distribution of the Ru reactants. Efficient energy migration makes electron injection rates relatively insensitive to the space distribution of the excited dye molecules.

We note that electron injection is always considerably faster than the respective back reaction, while the driving force for electron injection from the excited states ( $\Delta\epsilon^\circ = \epsilon^\circ(\text{Ru(II)}^*/\text{Ru(III)}) - \epsilon^\circ(\text{e}_{\text{TiO}_2^-}) = -0.85 - (-0.25) = 0.6$  V) is much smaller than that for the back reactions ( $\Delta\epsilon^\circ = \epsilon^\circ(\text{e}_{\text{TiO}_2^-}) - \epsilon^\circ(\text{Ru(II)/Ru(III)}) = 1.26 - (-0.25) = 1.51$  V). The value  $\epsilon^\circ = -0.25$  V has been estimated for surface-trapped electrons in TiO<sub>2</sub>.<sup>31</sup> Although the exact value depends on the specific conditions, the difference in driving force for electron injection and back reaction, 0.91 V in favor of the latter, does not depend on  $\epsilon^\circ(\text{e}_{\text{TiO}_2^-})$ . The inverted effect of the driving force on the reaction rates supports the conclusion that the space distribution of the Ru reactants plays a major role in determining the rates. Since the Ru(III) is more hydrophilic than the Ru(II), the balance between hydrophobic and ionic interactions is expected to be different during electron injection and back reaction. Consequently, the space distribution of the Ru complexes is also

different and the effects on electron injection and back reaction may not be similar.

**Specific Effects of SDS, SDBS, and Nafion on the Rates of Back Reactions.** The fastest part of the Ru(III)–electron recombination process, represented by reaction 7f, involves Ru(III) molecules that are in direct contact with the TiO<sub>2</sub> surface. The method used for preparation of the surfactant and polymer layers involves adsorption of the binder molecules, the ionic charge of which is opposite the TiO<sub>2</sub> surface charge, from acidic solutions. Excess Ru(II) was subsequently added at pH 2.5 in the absence of bulk surfactant. Under such conditions most of the SDS and SDBS negative charge is neutralized by the Ru(II), because there are no serious restrictions that may prevent diffusion of the dye molecules inside the TiO<sub>2</sub> membrane. Most of the surfactant molecules are expected to be in the form of Ru(II)(SDS)<sub>2</sub> or Ru(II)(SDBS)<sub>2</sub>, respectively. Formation of ion pairs is supported by the precipitation of SDS observed upon addition of stoichiometric amounts of SDS.<sup>62</sup> In homogeneous solutions, the precipitate redissolves upon further addition of SDS, upon reaching the cmc. Contact between the dye and TiO<sub>2</sub> may be either through a bpy (or o-phen) group of the dye or via SDS (or SDBS). This may cause the lifetime distribution of the recombination process.

Nafion is a partially cross-linked polymer, forming a membrane layer on the TiO<sub>2</sub> surface. The thickness of this layer, determined by the molecular dimensions of Nafion and by the pore size of the TiO<sub>2</sub> membrane, is on the order of 1 nm. Adsorption of the Nafion to TiO<sub>2</sub> involves predominantly interaction of the negative sulfonate groups with the positively charged TiO<sub>2</sub> surface. The ruthenium compounds are capable of diffusing through the Nafion and reaching the TiO<sub>2</sub> in sites where the positive surface charge has been neutralized by the Nafion. Electrostatic interactions between the Nafion and the dye molecules are possible despite the electrostatic TiO<sub>2</sub>/Nafion interactions,<sup>63</sup> causing location of the dye molecule at the interface. Dye molecules distributed at the surface may account for the fast component of the back reactions 7f, whereas molecules under stronger hydrophobic interactions and consequently further away from the surface are responsible for the longer lifetimes represented by reaction 7s.

Our results and conclusions are in qualitative agreement with Ford and Rodgers,<sup>53</sup> who investigated rates of back electron transfer reactions in SnO<sub>2</sub>/Ru(III)(bpy)<sub>2</sub>(bpy derivative) systems. The rates observed in this work are of the same order as in the earlier report, and the suggestion that electrostatic interactions between RuL<sub>3</sub> and the semiconductor surface influence the rates more than changes in the thermodynamic driving force<sup>53</sup> is in agreement with our conclusions.



**TABLE 9: Reaction Rate Constants of Adsorbed Ru(bpy)<sub>3</sub><sup>3+</sup> and Ru(o-phenyl)<sub>3</sub><sup>3+</sup> with I<sup>-</sup> Ions<sup>a</sup>**

system	iodide concentration	$k_{8f}$ (M <sup>-1</sup> s <sup>-1</sup> )	$k_{8s}$ (M <sup>-1</sup> s <sup>-1</sup> )
TiO <sub>2</sub> /SDS/Ru(bpy) <sub>3</sub> <sup>3+</sup> , wet	(1–5) × 10 <sup>-3</sup> M	(2.5 ± 1) × 10 <sup>8</sup>	(4.6 ± 1) × 10 <sup>7</sup>
TiO <sub>2</sub> /Nafion/Ru(bpy) <sub>3</sub> <sup>3+</sup> , wet	(1–5) × 10 <sup>-3</sup> M	(9 ± 2) × 10 <sup>8</sup>	(1.2 ± 0.4) × 10 <sup>8</sup>
TiO <sub>2</sub> /SDS/Ru(o-phen) <sub>3</sub> <sup>3+</sup> , wet	(1–2) × 10 <sup>-3</sup> M	(3.0 ± 0.8) × 10 <sup>8</sup>	(1 ± 0.5) × 10 <sup>8</sup>
TiO <sub>2</sub> /SDBS/Ru(o-phen) <sub>3</sub> <sup>3+</sup> , wet	(1–2) × 10 <sup>-3</sup> M	(6.0 ± 1.0) × 10 <sup>8</sup>	(7 ± 3) × 10 <sup>7</sup>
TiO <sub>2</sub> /Nafion/Ru(o-phen) <sub>3</sub> <sup>3+</sup> , wet	(2–4) × 10 <sup>-3</sup> M	(5.0 ± 1.0) × 10 <sup>8</sup>	(4.0 ± 1.5) × 10 <sup>7</sup>

<sup>a</sup> The signs “f” and “s” denote the fast and the slow oxidation of I<sup>-</sup>, respectively. Ground state absorbance at 460 nm was 0.5. Bleaching was measured at 420 nm. Second-order rate constants were calculated from the slopes of the linear plots of the pseudo-first-order rate constants vs [I<sup>-</sup>].

### Examination of the Ru(bpy)<sub>3</sub><sup>3+</sup> Results in the Dry Systems.

Comparison of  $k_{7f}$  shows that the highest rate is obtained in Nafion, in agreement with the suggestion that dye molecules bound primarily by ionic forces settle at the TiO<sub>2</sub>/Nafion interface. In contrast with the rigid structure of Nafion, SDS and SDBS molecules, which may be present in excess, are small enough to produce a strong local charge effect on Ru(III). Such interactions stabilize Ru(III) and slow down the rates of 7f. In addition, hydrophobic interactions in SDS involving the bpy ligand of Ru(bpy)<sub>3</sub><sup>3+</sup> and the alkyl segment of SDS are likely to keep the Ru(bpy)<sub>3</sub><sup>3+</sup> ions somewhat separated from the TiO<sub>2</sub> surface, decreasing the rate of reaction 7f compared with Nafion. Note that there is no distinct separation between hydrophobic and electrostatic zones, although the relative importance of the two types of interactions changes from site to site. Thus, increased contribution of hydrophobic interactions may slow reaction 7f without affecting the nature of the multiexponential distribution of lifetimes of the back reaction. SDBS is larger and more hydrophobic than SDS, and consequently  $k_{7f}$  is further lowered.

In Nafion, interactions with the perfluorinated alkyl chains remove the ruthenium complex molecules away from the electrostatic region at the TiO<sub>2</sub> surface, while in the SDS and SDBS systems a surfactant alkyl segment may separate between Ru(III) and the TiO<sub>2</sub>. In both cases, back reaction may still be possible because of segmental motion or tunneling.

**Ru(bpy)<sub>3</sub><sup>3+</sup> in the Wet Systems.** The presence of water decreases the ionic and increases the hydrophobic interactions of the surfactants/Nafion with the TiO<sub>2</sub> as well as with the dyes. This is reflected by a decreased rate of the charge recombination processes 7f and 7s (Table 6) in Nafion.

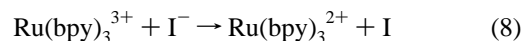
SDS and SDBS systems do not show a remarkable change: the respective rates in the dry and wet systems are comparable, although the water is expected to affect the ionic forces similarly to the effect in Nafion. Perhaps the increased mobility in the latter systems compensates for the reduced electrostatic interactions.

**Ru(o-phen)<sub>3</sub><sup>3+</sup>.** Under most studied conditions, the reactivity of Ru(o-phen)<sub>3</sub><sup>3+</sup> is comparable to that of Ru(bpy)<sub>3</sub><sup>3+</sup>. Exceptions are the dry Nafion system, where  $k_{7f}$  and  $k_{7s}$  are 4- and 2-fold lower, respectively, than in the Ru(bpy)<sub>3</sub><sup>3+</sup> systems (Table 7s). Note also that the value of  $k_{7f}$  in the Ru(o-phen)<sub>3</sub><sup>3+</sup>/Nafion is questionable in view of the poor separation between slow emission and fast bleaching rates. The above differences between the two photosensitizers are relatively small, although they may reflect the effect of increased hydrophobicity of Ru(o-phen)<sub>3</sub><sup>3+</sup>. The rates of the two ruthenium compounds in the SDS systems are comparable, with the only exception being the  $k_{7s}$  in the dry system. Although o-phenanthroline can be considered more hydrophobic than bipyridine, it is not clear whether the difference in hydrophobic interactions with the SDS alkyl segments is enough to produce a pronounced kinetic effect. Since the surfactant molecules point with their ionic groups toward the TiO<sub>2</sub> surface, the hydrophobic bindings with the alkyl groups may not be enough to remove the Ru(III) further from

the surface, and therefore the rates of both Ru compounds in the fast process may be comparable. On the other hand, the slower lifetimes represented by process 7s involve Ru(III) molecules removed from the surface because of stronger hydrophobic interactions. Ru(o-phen)<sub>3</sub><sup>3+</sup> may be further removed by its larger size, which affects the ionic charge density and increased number of alkyl chains between the dye and the TiO<sub>2</sub> surface, hence the lower reactivity of the o-phen complex in the slow process in the dry system.

The most pronounced difference between Ru(bpy)<sub>3</sub><sup>3+</sup> and Ru(o-phen)<sub>3</sub><sup>3+</sup> is observed in the SDBS systems. We suggest that specific hydrophobic interactions between Ru(o-phen)<sub>3</sub><sup>3+</sup> and the benzyl group of SDBS explain the enhanced relative reactivities of Ru(o-phen)<sub>3</sub><sup>3+</sup> observed in all systems. Since the benzyl group of SDBS is directly linked to the ionic sulfonate group, the combined ionic and hydrophobic interactions of this kind keep the Ru(o-phen)<sub>3</sub><sup>3+</sup> at or near the SDBS head under all conditions. Therefore, SDBS provides relatively higher rates, and in addition, the rate of recombination is only little affected by the presence of water.

**Reactions with Iodide Ions.** Iodide ions reduce Ru(III) back to Ru(II). A biexponential decay of the bleaching is observed (measured only in the wet systems), represented by reactions 8f and 8s (Table 9). The bpy and o-phen derivatives behave similarly. The iodine atom, which is the direct oxidation product, further reacts with iodide to form I<sub>2</sub><sup>-</sup>.<sup>61</sup> The latter disproportionates so that molecular iodine (in equilibrium with tri-iodide) is produced as the final stable product. None of the consecutive reactions are observed at 420 nm, where the bleaching kinetics is measured. The second-order values of  $k_{8f}$  and  $k_{8s}$  are summarized in Table 9, where the reaction rate constants have been derived from slopes of the respective pseudo-first-order rate constants when plotted vs [I<sup>-</sup>]. Note that  $k_{8f}$  values are 3–12 times higher than the respective values of  $k_{8s}$ . The relatively rapid reactions with I<sup>-</sup> indicate that the layers



formed upon addition of the surfactants or the Nafion are indeed very thin, so that the iodide ions can easily reach the Ru(III). It is thus possible to rule out that the surfactants form micellar-like structures at the TiO<sub>2</sub> surface, in which case the ionic charge of the surfactant molecules is expected to repel the negatively charged iodide and inhibit its reactions with Ru(III).

Oxidation of iodide by Ru(bpy)<sub>3</sub><sup>3+</sup> in homogeneous solution ( $k = 1 \times 10^5 \text{ M}^{-1} \text{ s}^{-1}$ ) and by Ru(bpy)<sub>2</sub>(bpy(C<sub>19</sub>H<sub>39</sub>))<sub>2</sub><sup>3+</sup> monolayer ( $k = 2.5 \times 10^4 \text{ M}^{-1} \text{ s}^{-1}$ ) is much slower than in the present work.<sup>65</sup> This observation may indicate that iodide ions may settle at the TiO<sub>2</sub> surface, possibly because of a residual positive surface charge. This would enhance their oxidation by Ru(III).

In contrast to the efficient reaction 8, iodide ions have only a small effect on the lifetime of the excited states of Ru(bpy)<sub>3</sub><sup>2+</sup> and Ru(o-phen)<sub>3</sub><sup>2+</sup> (see Table 10). Thus, with the exception of the SDS–Ru(bpy)<sub>3</sub><sup>2+</sup> system (where the lifetimes of the

**TABLE 10: Effect of Iodide on Emission Decay Rates<sup>a</sup>**

system	$\times 10^{-6} \text{ s}^{-1}$	
	$k_2$	$k_3$
TiO <sub>2</sub> /SDS/Ru(bpy) <sub>3</sub> <sup>2+</sup> , 0.1 M KI	2.9	42
TiO <sub>2</sub> /SDBS/Ru(bpy) <sub>3</sub> <sup>2+</sup> , 0.1 M KI	2.0	22
TiO <sub>2</sub> /Nafion/Ru(bpy) <sub>3</sub> <sup>2+</sup> , 0.25 M KI	2.7	18
TiO <sub>2</sub> /SDS/Ru(o-phen) <sub>3</sub> <sup>2+</sup> , 0.15 M KI	1.1	10
TiO <sub>2</sub> /SDBS/Ru(o-phen) <sub>3</sub> <sup>2+</sup> , 0.1 M KI	1.6	20
TiO <sub>2</sub> /Nafion/Ru(o-phen) <sub>3</sub> <sup>2+</sup> , 0.15 M KI	2.9	19

<sup>a</sup> pH 2.5,  $\sim 4 \times 10^{-10}$  einsteins absorbed per cm<sup>2</sup>. Rate constants other than  $k_2$  and  $k_3$  are the average values computed in the respective KI-free systems.

exponential decays of emission are shortened by 30–50% upon addition of 0.1 M iodide) very little or no quenching takes place at iodide concentration below 0.1 M. This apparent contrast is a result of a combination of reasons: (a) Iodide has a relatively low reactivity toward Ru(II) triplets in homogeneous solutions as well.<sup>66</sup> (b) The short lifetime of the excited dyes in comparison with the lifetime of the Ru(III) makes the competition of iodide for Ru(III) relatively more effective. (c) Ru(III) ions possess three positive charges, while the Ru(II) are only doubly charged. This is expected to make the Ru(III) complexes more accessible to iodide ions, because of the higher local positive charge at the reaction site. (d) The higher hydrophobicity of the Ru(II) complexes further decreases their accessibility to the I<sup>−</sup> ions.

**Surface Energy Migration and Triplet–Triplet Annihilation.** The second-order components of emission decay that compete with the exponential decays at high laser intensities are attributed to triplet–triplet annihilation. Triplet–triplet annihilation of \*Ru(bpy)<sub>3</sub><sup>2+</sup> was reported for both micelle (SDS) and polyelectrolyte (polyvinyl sulfate) systems.<sup>67,68</sup> Previously investigated semiconductor systems were studied using low steady state light intensities (e.g. those that are used for measurements of photocurrents) or had very rapid electron injection rates, which prevented accumulation of sufficiently high densities of triplets which could lead to triplet–triplet annihilation.

Under our conditions, the highest laser pulse intensity is 103 times higher than the lowest, but the initial emission intensities change by a factor of 30–50 only. This apparent discrepancy results in part from bleaching of the ground states of the dyes. In a typical experiment (absorbance of Ru(bpy)<sub>3</sub><sup>2+</sup> at 452 nm prior to the laser pulse equals 0.5), the concentration of the dye is  $3.4 \times 10^{-8}$  mol/cm<sup>2</sup>. At the highest laser light intensity, the amount of absorbed excitation light (based on the prepulse absorbance) is  $(2-3) \times 10^{-8}$  einsteins/cm<sup>2</sup>, corresponding to depletion of 20–25% of the dye during the laser pulse. Thus, bleaching has a considerable effect on the absorbed light. In addition a small fraction of the excited dye molecules decay by the bimolecular reaction 5 within the time resolution of the system (about 10 ns). However, two observations cannot be explained by these two effects alone: (a) Except for the two lowest intensities, the emission signals increase much less than linearly with the excitation light intensities even after correction for ground state bleaching. (b) The fast bimolecular decay within the time resolution of the measurements may affect only the fast decay, in which case the observed initial ratio [ $\text{*Ru(bpy)}_3^{2+}$ ]<sub>0</sub>/[ $\text{*Ru(bpy)}_3^{2+}$ ]<sub>f</sub> is expected to increase with pulse intensity. However, this is in contrast to most observations (see Tables 1s–4s). To explain these observations it is suggested that certain zones of the surface contain particularly high concentrations of dye molecules and that very fast triplet annihilation involves efficient energy migration within these zones. As a result, the “initial” emission decays before any

data can be recorded. This process takes place both with (\*Ru(bpy)<sub>3</sub><sup>2+</sup>)<sub>f</sub> and (\*Ru(bpy)<sub>3</sub><sup>2+</sup>)<sub>s</sub> and their o-phen analogues.

An interesting observation is the similar behavior of the dry and wet systems. The rate constants in a given system change by no more than a factor of  $\sim 2$  (with the exception of the wet TiO<sub>2</sub>/Nafion/Ru(o-phen)<sub>3</sub><sup>2+</sup>, for which no bimolecular reactions could be measured). Since no diffusion is possible in the dry systems, the second-order decay reactions must be attributed to efficient energy transfer. The similarity between the results of the dry and wet systems suggests that energy migration is important in the wet systems as well. Efficient energy migration is possible only at high dye densities. The thickness of a typical TiO<sub>2</sub> layer was between 4 and 5  $\mu\text{m}$  (calculated from the weight of TiO<sub>2</sub>, assuming dense packing of TiO<sub>2</sub> nanocrystallites in the layers). Since about 70% of the volume is occupied by the TiO<sub>2</sub> nanocrystallites, the average distance between two dye molecules within the remaining volume can be calculated as 2 nm. In fact, the actual distance must be considerably smaller because of the relatively large size of the dye–surfactant ion pair (diameter  $\approx 1$  nm), which is expected to increase the excluded volume. Consequently, at least a major fraction of the dye molecules must be in close contact, allowing energy migration effects as discussed above. Again, the differences between  $k_4$  and  $k_5$  are attributed to the lifetime distribution related to the distribution of distances between the reacting species.

## Conclusions

Adsorption of the positive ions Ru(bpy)<sub>3</sub><sup>2+</sup> and Ru(o-phen)<sub>3</sub><sup>2+</sup> to the surface of TiO<sub>2</sub> at pH 2.5, where the TiO<sub>2</sub> nanocrystallites are positively charged, occurs upon pretreatment of the surface with appropriate surfactants and polymers. The uptake of the dyes per given amount of TiO<sub>2</sub> is only 4 times less than reported for the TiO<sub>2</sub>/Ru(dcbpy)<sub>2</sub>CNS)<sub>2</sub> system, although the latter adsorbs directly to the nanocrystallites' surface.

Our work shows that at relatively low laser pulse intensities electron injection competes with self-decay of the excited states.

At high laser intensities efficient triplet decay involving very fast energy migration takes place. Both the electron injection processes and the electron recapture reactions obey biexponential rate laws, which account for nearly all the reactants' concentrations. The nature of binding of the photosensitizers, involving both electrostatic and hydrophobic forces, affects the average distances between the excited dye and the TiO<sub>2</sub> surface.

**Acknowledgment.** This work was supported by the Institute of Physical and Chemical Research, the Israeli Ministry of Energy, and the Farkas Center for Light Induced Processes. One of us (J.R.) wishes to express his gratitude to the Institute of Physical and Chemical Research for his invitation within the frame of the PS program. We are indebted to Prof. G. Czapski (Hebrew University) and Prof. M. Hoffmann (Caltech) for useful discussions.

**Supporting Information Available:** Figures 1s and 3s and Tables 1s, 2s, 3s, 4s, 6s, and 7s (9 pages). Ordering information is given on any current masthead page.

## References and Notes

- Hagfeldt, A.; Graetzel, M. *Chem. Rev.* **1995**, 95, 49–68.
- Hagfeldt, A.; Lindquist, S.-E.; Graetzel, M. *Sol. Energy Mater. Sol. Cells* **1994**, 32, 245–57.
- McEvoy, A. J.; Graetzel, M. *Sol. Energy Mater. Sol. Cells* **1994**, 32, 221–7.
- Kay, A.; Humphry-Baker, R.; Graetzel, M. *J. Phys. Chem.* **1994**, 98, 952–9.

- (5) Nazeeruddin, M. K.; Kay, A.; Rodicio, I.; Humphry-Baker, R.; Mueller, E.; Liska, P.; Vlachopoulos, N.; Graetzel, M. *J. Am. Chem. Soc.* **1993**, *115*, 6382–90.
- (6) O'Regan, B.; Graetzel, M. *Nature (London)* **1991**, *353*, 737–40.
- (7) Smestad, G. *Sol. Energy Mater. Sol. Cells* **1994**, *32*, 273–88.
- (8) Smestad, G.; Bignozzi, C. A.; Argazzi, R. *Sol. Energy Mater. Sol. Cells* **1994**, *32*, 259–72.
- (9) Smestad, G.; Ries, H. *Sol. Energy Mater. Sol. Cells* **1992**, *25*, 51–71.
- (10) Argazzi, R.; Bignozzi, C. A.; Heimer, T. A.; Castellano, F. N.; Meyer, G. *J. Inorg. Chem.* **1994**, *33*, 5741–9.
- (11) Dabestani, R.; Bard, A. J.; Campion, A.; Fox, M. A.; Mallouk, T. E.; Webber, S. E.; White, J. M. *J. Phys. Chem.* **1988**, *92*, 1872–8.
- (12) Fitzmaurice, D. J.; Frei, H. *Langmuir* **1991**, *7*, 1129–37.
- (13) (a) Gerischer, H.; Lubke, M. *J. Electroanal. Chem.* **1986**, *204*, 225–7. (b) Vogel, R.; Hoyer, P.; Weller, H. *J. Phys. Chem.* **1994**, *98*, 3183–8.
- (14) Henglein, A.; Gutierrez, M.; Weller, H.; Fojtik, A.; Jirkovsky, J. *Ber. Bunsen-Ges. Phys. Chem.* **1989**, *93*, 593–600.
- (15) Henglein, A.; Weller, H. In *Photochemical Energy Conversion*; Norris, J. R., Jr., Meisel, D., Eds.; Elsevier: New York, 1989; pp 161–72.
- (16) Henglein, A. *Topics in Current Chemistry*; Steckhan, E., Ed.; Springer-Verlag: Berlin, 1988; Vol. 143, pp 113–80.
- (17) Henglein, A. *Prog. Colloid Polym. Sci.* **1987**, *73*, 1–4.
- (18) Electron injection from illuminated CdS into attached TiO<sub>2</sub> and ZnO particles. Spanhel, L.; Weller, H.; Henglein, A. *J. Am. Chem. Soc.* **1987**, *109*, 6632–5.
- (19) Spanhel, L.; Henglein, A.; Weller, H. *Ber. Bunsen-Ges. Phys. Chem.* **1987**, *91*, 1359–63.
- (20) Spanhel, L.; Weller, H.; Fojtik, A.; Henglein, A. *Ber. Bunsen-Ges. Phys. Chem.* **1987**, *91*, 88–94.
- (21) Weller, H.; Schmidt, H. M.; Koch, U.; Fojtik, A.; Baral, S.; Henglein, A.; Kunath, W.; Weiss, K.; Dieman, E. *Chem. Phys. Lett.* **1986**, *124*, 557–60.
- (22) Baral, S.; Fojtik, A.; Weller, H.; Henglein, A. *J. Am. Chem. Soc.* **1986**, *108*, 375–8.
- (23) Koch, U.; Fojtik, A.; Weller, H.; Henglein, A. *Chem. Phys. Lett.* **1985**, *122*, 507–10.
- (24) Fojtik, A.; Weller, H.; Henglein, A. *Chem. Phys. Lett.* **1985**, *120*, 552–4.
- (25) Weller, H.; Fojtik, A.; Henglein, A. *Chem. Phys. Lett.* **1985**, *117*, 485–8.
- (26) Fojtik, A.; Weller, H.; Koch, U.; Henglein, A. *Ber. Bunsen-Ges. Phys. Chem.* **1984**, *88*, 969–77.
- (27) Gopidas, K. R.; Bohorquez, M.; Kamat, P. V. *J. Phys. Chem.* **1990**, *94*, 6435–40.
- (28) Fitzmaurice, D., J.; Frei, H.; Rabani, J. *J. Phys. Chem.* **1995**, *99*, 9176–81.
- (29) Rabani, J. *J. Phys. Chem.* **1989**, *93*, 7707–13.
- (30) Martin, S. T.; Herrmann, H.; Choi, W.; Hoffmann, M. R. *J. Chem. Soc., Faraday Trans.* **1994**, *90*, 3315–22.
- (31) Martin, S. T.; Herrmann, H.; Hoffmann, M. R. *J. Chem. Soc., Faraday Trans.* **1994**, *90*, 3323–30.
- (32) Micic, O. I.; Rajh, T.; Nedeljkovic, J. M.; Comor, M. I. *Isr. J. Chem.* **1993**, *33*, 59–65.
- (33) Nosaka, Y.; Fukuyama, T.; Horiuchi, M.; Fujii, N. *Isr. J. Chem.* **1993**, *33*, 71–5.
- (34) Mulvaney, P.; Grieser, F.; Meisel, D. *Langmuir* **1990**, *6*, 567–72.
- (35) Liu, D.; Kamat, P. V. *J. Electrochem. Soc.* **1995**, *142*, 835–9.
- (36) Bedja, I.; Hotchandani, S.; Kamat, P. V. *J. Phys. Chem.* **1994**, *98*, 4133–40.
- (37) Bedja, I.; Hotchandani, S.; Carpentier, R.; Vinodgopal, K.; Kamat, P. V. *Thin Solid Films* **1994**, *247*, 195–200.
- (38) Vinodgopal, K.; Kamat, P. V. *Environ. Sci. Technol.* **1995**, *29*, 841–5.
- (39) Bjorksten, U.; Moser, J.; Graetzel, M. *Chem. Mater.* **1994**, *6*, 858–63.
- (40) Gershuni, S.; Stark, J.; Rabani, J. To be published.
- (41) Rabani, J.; Behar, D. *J. Phys. Chem.* **1989**, *93*, 2559–63.
- (42) Yoneyama, H. *Res. Chem. Intermed.* **1991**, *15*, 101–11.
- (43) Nakabayashi, S.; Amemiya, T.; Kira, A. *J. Phys. Chem.* **1992**, *96*, 2272–4.
- (44) Rajh, T.; Rabani, J. *Langmuir* **1991**, *7*, 2054–9.
- (45) *Photochemical Conversion and Storage of Solar Energy*; Pelizzetti, E., Schiavello, M., Eds.; Kluwer Acad. Publishers: Dordrecht, 1991; pp 103–19.
- (46) (a) Yoshimura, A.; Hoffman, M. Z.; Sun, H. *J. Photochem. Photobiol. A* **1993**, *70*, 29–33. (b) James, D. R.; Liu, Y. S.; Mayo, P. D.; Ware, W. R. *Chem. Phys. Lett.* **1985**, *120*, 460. (c) Lin, R.-J.; Onikubo, T.; Nagai, K.; Kaneko, M. *J. Electroanal. Chem.* **1993**, *348*, 189–99.
- (47) Lin, R.-J.; Onikubo, T.; Nagai, K.; Kaneko, M. *J. Electroanal. Chem.* **1993**, *348*, 189–99.
- (48) Moser, J.; Graetzel, M. *J. Am. Chem. Soc.* **1984**, *106*, 6557–64.
- (49) (a) Hashimoto, K.; Hiramoto, M.; Kajiwara, T.; Sakata, T. *J. Phys. Chem.* **1988**, *92*, 4636–40. (b) Hashimoto, K.; Hiramoto, M.; Lever, A. B. P.; Sakata, T. *J. Phys. Chem.* **1988**, *92*, 1016–8.
- (50) Eichberger, R.; Willig, F. *Chem. Phys.* **1990**, *141*, 159–73.
- (51) Vinodgopal, K.; Hua, X.; Dahlgren, R. L.; Lappin, A. G.; Patterson, L. K.; Kamat, P. V. *J. Phys. Chem.* **1995**, *99*, 10883–9.
- (52) (a) Fessenden, R. W.; Kamat, P. V. *J. Phys. Chem.* **1995**, *99*, 12902–6. (b) Kamat, P. V.; Bedja, I.; Hotchandani, S.; Patterson, L. K. *J. Phys. Chem.* **1996**, *100*, 4900–8. (c) Vinodgopal, K.; Hua, X.; Dahlgren, R. L.; Lappin, A. G.; Patterson, L. K.; Kamat, P. V. *J. Phys. Chem.* **1995**, *99*, 10883–9.
- (53) Ford, W. E.; Rodgers, M. A. J. *J. Phys. Chem.* **1994**, *98*, 3822–31.
- (54) (a) Kamat, P. V. *Langmuir* **1990**, *6*, 512. (b) Kamat, P. V.; Das, S.; Thomas, K. J.; George, M. V. *Chem. Phys. Lett.* **1991**, *178*, 75. (c) Willig, F.; Eichberger, R.; Sundaresan, N. S.; Parkinson, B. A. *J. Am. Chem. Soc.* **1990**, *112*, 2702.
- (55) (a) Kemnitz, T.; Murao, I.; Yamazaki, N.; Nakashima, N.; Yoshihara, K. *Chem. Phys. Lett.* **1983**, *101*, 337. (b) Willig, F.; Blumen, A.; Zumofen, G. *Chem. Phys. Lett.* **1984**, *108*, 222. (c) Anfinrud, P.; Crackel, R. L.; Struve, W. S. *J. Phys. Chem.* **1984**, *88*, 5873.
- (56) Slama-Schwok, A.; Rabani, J. *Macromolecules* **1988**, *21*, 764–8.
- (57) Meisel, D.; Rabani, J.; Meyerstein, D.; Matheson, M. S. *J. Phys. Chem.* **1978**, *82*, 985–90.
- (58) For review see: *Photocatalysis, Fundamentals and Applications*; Serpone, N.; Pelizzetti, E., Eds.; Wiley: New York, 1989.
- (59) Juris, A.; Balzani, V. *Coord. Chem. Rev.* **1988**, *84*, 85–277.
- (60) Kormann, C.; Bahnemann, D. W.; Hoffmann, M. R. *J. Phys. Chem.* **1988**, *92*, 5196.
- (61) Grossweiner, L. I.; Matheson, M. S. *J. Phys. Chem.* **1957**, *61*, 1089.
- (62) Meisel, D.; Matheson, M. S.; Rabani, J. *J. Am. Chem. Soc.* **1978**, *100*, 117.
- (63) Nahor, G. S.; Rabani, J. *Macromolecules* **1989**, *22*, 2516–19.
- (64) Yoshimura, A.; Hoffman, M. Z.; Sun, H. *J. Photochem. Photobiol. A* **1993**, *70*, 29–33.
- (65) Rabani, J.; Hashimoto, K.; Liu, Z. F.; Fujishima, A. *Langmuir* **1993**, *9*, 1818–23.
- (66) Demas, J. N.; Adington, J. W.; Peterson, S. H.; Harris, E. W. *J. Phys. Chem.* **1977**, *81*, 1039.
- (67) Lachish, U.; Ottolenghi, M.; Rabani, J. *J. Am. Chem. Soc.* **1977**, *99*, 8062–3.
- (68) Kelder, S.; Rabani, J. *J. Phys. Chem.* **1981**, *85*, 1637–40.